

Ground Motions from the 7 and 19 September 2017 Tehuantepec and Puebla-Morelos, Mexico, Earthquakes

by Valerie J. Sahakian,* Diego Melgar, Luis Quintanar, Leonardo Ramírez-Guzmán, Xyoli Pérez-Campos, and Annemarie Baltay

Abstract The 2017 M 8.2 Tehuantepec and M 7.1 Puebla-Morelos earthquakes were deep inslab normal-faulting events that caused significant damage to several central-to-southern regions of Mexico. Inslab earthquakes are an important component of seismicity and seismic hazard in Mexico. Ground-motion prediction equations (GMPEs) are an integral part of seismic hazard assessment as well as risk and rapid-response products. This work examines the observed ground motions from these two events in comparison to the predicted median ground motions from four GMPEs. The residuals between the observed and modeled ground motions allow us to study regional differences in shaking, the effects of each earthquake, and basin effects in Mexico City, Puebla, and Oaxaca. We find that the ground motions from these two earthquakes are generally well modeled by the GMPEs. However, the Tehuantepec event shows larger than expected ground motions at greater distances and longer periods, which suggests a waveguide effect from the subduction zone geometry. Finally, Mexico City and the cities of Puebla and Oaxaca exhibit very large ground motions, indicative of well-known site and basin effects that are much stronger than the basin terms included in some of the GMPEs. Simple and rapid ground-motion parameter estimates that include site effects are key for hazard and real-time risk assessments in regions such as Mexico, where the vast majority of the population lives in areas where the aforementioned effects are relevant. However, GMPEs based on site correction terms dependent on topographic slope proxies underestimate, at least in the three cities tackled in this work, the observed amplification. Therefore, there is a need to improve models of seismic amplification in basins that could be included in GMPEs.

Electronic Supplement: Tables of ground-motion intensity measures for each station and earthquake, as well as the residual uncertainties for each model, over all distances, and figures showing comprehensive ground-motion prediction equation (GMPE) and residuals results, for every period considered in this study, and the uncertainties.

Introduction

The subduction of the Cocos plate beneath the North American plate yields a complicated tectonic environment. The dip of the subducting plate varies dramatically, from a flat slab underneath central Mexico to steeply dipping subduction underneath the state of Oaxaca and southward to central America (Fig. 1, [Pardo and Suárez, 1995](#)). This dramatic variation produces a large diversity of stress regimes and faulting styles over a broad region (e.g., [Pacheco and Singh, 2010](#)). As a result, seismic hazard in Mexico arises

from a combination of interface megathrust events, inslab normal- and thrust-faulting events, and continental events (e.g., [Shedlock, 1999](#)); all of these mechanisms are capable of producing damage to nearby population centers ([García-Acosta and Suárez, 1996](#)). Within this context, two large inslab events occurred in September 2017. The M 8.2 Tehuantepec earthquake of 8 September was a large offshore event, landward of the trench, with a high-angle (70° – 80° dip) normal-faulting focal mechanism ([Ye et al., 2017](#)). Unlike previous large (M 7.8+) normal-faulting events worldwide (e.g., [Okal et al., 2016](#)), the 8 September 2017 M 8.2 Tehuantepec event ruptured almost all of the oceanic

*Now at Department of Earth Sciences, University of Oregon, 1585 East 13th Avenue, Eugene, Oregon 97403.

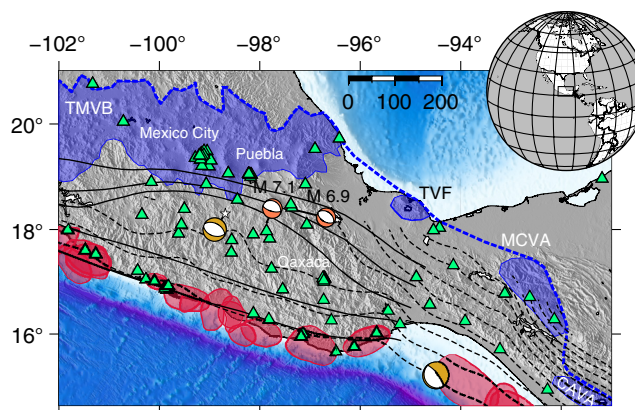


Figure 1. Regional map for this study. The larger focal mechanisms show the hypocentral location and moment tensor for the Puebla-Morelos and Tehuantepec earthquakes. Smaller, labeled focal mechanisms are for older normal-faulting inslab events. Stations included in this study are shown as triangles. Solid lines show the 20, 40, 60, 80, and 100 km slab contours compiled by Ferrari *et al.* (2012). Dashed lines are the slab contours at the same intervals but from Slab 1.0 (Hayes *et al.*, 2012). In the flat slab portion, the Ferrari *et al.* (2012) model is constrained by the receiver-function result by Pérez-Campos *et al.* (2008), and therefore a preferred interpretation. Thick dashed lines show the delineation used to define stations as fore-arc or back-arc for the BC Hydro ground-motion prediction equation (GMPE). Shaded regions on the Pacific coast show historical rupture extents; shaded regions in the north delineate volcanic regions. Mexico City, Puebla, and Oaxaca are labeled. The globe in the upper right shows the figure location with a dark rectangle. TVF, Los Tuxtlas volcanic field; MCVA, modern Chiapanean volcanic arc; CAVA, central American volcanic arc. The color version of this figure is available only in the electronic edition.

lithosphere, with centroid moment release at 54 km depth and slip from 10 km down to at least 80 km depth (Melgar, Ruiz-Angulo, *et al.*, 2018). The M 7.1 Puebla-Morelos event occurred 11 days later on 19 September, ~600 km northwest of the Tehuantepec earthquake, at a depth of 57 km. At 260 km from the trench, it is much farther inland, located in the transition between flat-slab subduction and steeply dipping subduction (Fig. 1). In this region, the slab dip angle changes by as much as 70° over a very short distance: it is likely that the Puebla-Morelos earthquake was the result of large bending stresses (Melgar, Pérez-Campos, *et al.*, 2018). However, unlike the Tehuantepec event, the Puebla-Morelos earthquake only ruptured the subducted oceanic crust and the top portion of the oceanic mantle, and thus broke only the top half of the lithosphere, which is expected to be in flexure-driven extension.

Although both earthquakes were damaging, the 19 September 2017 M 7.1 Puebla-Morelos earthquake was much closer to the heavily urbanized part of the country, which includes major population centers such as Mexico City, Puebla, and the city of Cuernavaca. In Mexico City, structural building damage and loss of life were concentrated mostly in the lake and partially in the transition geotechnical zones, according to Mexico's capital building provision, the 2004 Complementary Technical Norms (Gobierno del Distrito

Federal [GDF], 2004; Çelebi *et al.*, 2018), in soils with fundamental periods between 1.0 and 1.5 s. At least 46 structures collapsed and many hundreds more were damaged, and 246 casualties were reported (Mayoral-Villa *et al.*, 2017). The Puebla-Morelos earthquake is the most significant earthquake to affect central Mexico since the 19 September 1985 M_s 8.1 Michoacán earthquake—a large megathrust event far from the city, which led to an estimated 10,000–20,000 casualties (Universidad Nacional Autónoma de México [UNAM] Seismology Group, 1986).

Background

Damaging inslab normal-faulting events are not uncommon in Mexico. Previous damaging inslab earthquakes include the 1931 M_s 8.0 Oaxaca earthquake, which occurred on a high angle normal fault just west of the 2017 Tehuantepec event and was also hypothesized to break most of the lithosphere (Singh *et al.*, 1985), and the 1999 M 7.0 Tehuacan earthquake 150 km west of the 2017 Puebla-Morelos event (Fig. 1, Singh *et al.*, 1999). These two earthquakes, similar to the 2017 events, demonstrate that inslab normal-faulting events in the Mexican subduction zone can be separated into two groups. First, in central Mexico, earthquakes such as the 2017 M 7.1 Puebla-Morelos and 1999 M 7.0 Tehuacan events that are likely the result of large bending stresses in the region of rapid transition from flat slab to steep subduction (Melgar, Pérez-Campos, *et al.*, 2018, Fig. 1). Second, events such as the 1931 Oaxaca and 2017 Tehuantepec earthquakes, which occur in the Oaxaca and Chiapas regions of southern Mexico that may be driven by a breakdown or detachment of the entire slab (e.g., Ye *et al.*, 2017). This breakdown might be the result of strong normal stresses within it (slab pull) and other structural considerations such as the fabric of the incoming seafloor (e.g., Melgar, Ruiz-Angulo, *et al.*, 2018).

Although a large component of seismic hazard in this region is driven by megathrust events (Zúñiga *et al.*, 1997; Pozos-Estrada *et al.*, 2014; Comisión Federal de Electricidad [CFE], 2015), the 7 September 2017 M 8.2 Tehuantepec and 19 September 2017 M 7.1 Puebla-Morelos normal-faulting, inslab earthquakes are a stark reminder that other mechanisms contribute to the hazard. In fact, disaggregating the hazard at rock sites shows that at distances < 200 km (i.e., the Puebla-Morelos earthquake to Mexico City) and frequencies larger than 1 Hz, inslab events dominate in many of the largest population centers such as Mexico City. In turn, an event such as the Tehuantepec earthquake, which occurred more than 500 km away from the capital, represents only a small component of the city's seismic hazard; at this distance, subduction zone events represent a far larger component of total hazard (Pozos-Estrada *et al.*, 2014). Thus, it is important to understand the nature of seismic sources in the region, and their effects regionally as well as in highly populated areas.

A key component of such hazard calculations is the estimation of expected ground motions, typically modeled by ground-motion prediction equations (GMPEs). Typically,

GMPEs provide an empirical estimation of the median expected ground motion, and the expected standard deviation, in a given region. In this work, we analyze the ground motions from the two recent September 2017 earthquakes and study how well they are or are not modeled by current GMPEs. Considering differences between observed ground motions and predictions (i.e., residuals, in the terminology of GMPEs) yields information not only about attenuation in the region but also about the earthquake and site effects. In addition, this comparison can aid in determining which GMPEs are the most appropriate model for the region of interest.

The utility of such efforts was recently highlighted by [Baltay and Boatwright \(2015\)](#) who performed a similar analysis for the 2014 M 6.0 Napa, California, earthquake and compared the observed ground motions to the GMPEs for California ([Bozorgnia et al., 2014](#)). Even within a comparatively narrow geographic region, there was large spatial variation in the ground-motion residuals from the Napa event, demonstrating the need for ground-motion models that are more regionalized than the existing models. In addition, they found that the event had an average stress drop in comparison to the GMPEs (i.e., average with respect to the dataset on which the GMPEs were developed), and that there likely exists waveguide effects in the region.

From the first nationwide hazard map ([Esteva, 1968, 1970](#)) to the latest estimate in the Seismic Design Chapter of the MDOC-2015 ([CFE, 2015](#)), a variety of GMPEs have been used in Mexico. The current version of the MDOC-2015 hazard map uses the [Arroyo et al. \(2010\)](#), [Zhao et al. \(2006\)](#), and [Abrahamson and Silva \(1997\)](#) GMPEs for interplate, intraslab, and shallow crustal earthquakes, respectively. Paired with a substantial increment in the seismic instrumentation, the two events discussed in this research provide a good testing ground for intraplate ground-motion models.

In our study, we investigate how well existing GMPEs model ground motions in the region. We focus on regional patterns in the differences between GMPE predictions and observations (the residuals), and how those patterns may be controlled by the geological structure of central and southern Mexico. Furthermore, we consider these residuals for recordings in basins in the cities of Mexico (Mexico City, Puebla, and Oaxaca) because a large proportion of population resides, in numbers and density, in these basins. We observe large amplifications and study how well GMPEs model the amplification. Finally, we discuss the implications of these results on hazards for the country, and how this may be used to improve models of both hazard and risk, going forward.

Methods

To study ground-motion residuals, we rely on strong-motion recordings for each earthquake, using observations from a federated set of networks that spans Mexico. We use three component strong-motion recordings from the Servicio Sismológico Nacional, a part of the Instituto de Geofísica (IG) at the UNAM, as well as from the Unidad de Instrumen-

tación Sísmica at the Instituto de Ingeniería also within UNAM, and from a research network, the Red Sísmica del Valle de México, which has strong-motion sensors within Mexico City and is also operated by IG and UNAM. We compare these observations to four different models of ground motion that specifically account for inslab earthquakes in subduction zones.

Ground-Motion Data and Processing

Seismic data from any available UNAM strong-motion stations are processed and only stations within 700 km of each earthquake are included in the analysis. At this distance, visual inspection still yielded very clear arrivals of the events. This yields 78 stations for the M 8.2 Tehuantepec earthquake at rupture distances from 40 to 655 km, and 74 for the Puebla-Morelos earthquake, at rupture distances from 57 to 655 km. The data are corrected for instrument response, and high-pass filtered with a 20 s filter corner to remove baseline offsets. We used a fixed time-window length for each event: for the Tehuantepec earthquake, we consider 180 s of data after the first arrival; for the Puebla-Morelos earthquake, we use 120 s. Visual inspection of the closest recordings to the source reveals no obvious early aftershocks that could contaminate the results. The two horizontal components of ground motion are combined into the orientation independent nongeometric mean (RotD50) method ([Boore 2010](#)). Using PyRotD ([Kottke, 2017](#)), we compute peak ground acceleration (PGA) and the 5% damped response spectral accelerations for oscillator periods of 5.0, 4.0, 2.0, 1.0, 0.5, 0.2, and 0.1 s; we select these periods because they are common to the four GMPEs considered in this study. PGV was not common to all GMPEs, and as such is not included in this analysis. These ground-motion intensity values are included in [Tables S1 and S2](#) (available in the electronic supplement to this article) for the Tehuantepec and Puebla-Morelos events, respectively.

Ground-Motion Prediction Equations

A total of four GMPEs are considered in this study: first, a regional GMPE developed with data from inslab events in Mexico ([García et al., 2005](#)). Second and third, a GMPE developed for Japan that can be used to independently estimate ground motions for active-shallow crust (ASC) and intraslab (SSLab) events ([Zhao et al., 2006](#)); we test both implementations of the GMPE. Finally, we use a subduction zone GMPE developed for the Cascadia subduction zone referred to as BC Hydro, which also specifically accounts for inslab events ([Abrahamson et al., 2016](#)). A comparison of the basic features of these GMPEs can be found in Table 1. Predictions for these four ground-motion models are computed within a consistent framework using the open-source software OpenQuake ([Pagani et al., 2014](#)), developed by the Global Earthquake Model Foundation.

The [García et al. \(2005\)](#) GMPE is specifically designed from data for intermediate depth (between 35 and 138 km),

Table 1
Qualitative Comparison of Ground-Motion Prediction Equations for Each Considered in This Study

Model	Data Used in Model Development	Distances (km)	Magnitudes	Site Effects	Other Notes
García <i>et al.</i> (2005)	16 events from central Mexico	< 400	5.2 < M < 7.4	All sites assumed to be NEHRP class B	35 < depth < 138 km
Zhao <i>et al.</i> (2006)	Japan, western United States, Iran; 4726 records total	< 300	4.9 < M < 8.5	Four classifications: rock, hard soil, medium soil, and soft soil	10 < focal depth < 130 km; ASC vs. slab source classification
Abrahamson <i>et al.</i> (2016) BC Hydro Inslab	2590 recordings of 63 slab events (Alaska, Cascadia, Japan, Taiwan, south and central America, and Mexico)	< 300	5.0 < M < 7.9 (for slab events)	Nonlinear V_{S30} site effects	Fore-arc vs. back-arc classification for attenuation

NEHRP, National Earthquake Hazards Reduction Program; ASC, active-shallow crust.

normal-faulting inslab events in central Mexico such as the Tehuantepec and Puebla-Morelos events (Table 1). The dataset used to derive the GMPE was constrained to $5.2 < M_w \leq 7.4$ and regional distances below 400 km. It has no site-effect term and assumes all sites are rock (i.e., National Earthquake Hazards Reduction Program [NEHRP] B classification; $760 \text{ m/s} < V_S \leq 1500 \text{ m/s}$, Building Seismic Safety Council [BSSC], 2004). This model includes a magnitude scaling term, geometrical spreading, and intrinsic attenuation terms, as well as a focal depth term.

Designed for Japan, the Zhao *et al.* (2006) models (Table 1) predict ground motions for interface, ASC, and inslab (SSlab) events separately, and was developed on data of distances less than 300 km. They assume that each type of event exhibits different attenuation as a function of distance. Zhao *et al.* (2006) includes four site classes used in Japanese engineering design: rock, hard soil, medium soil, and soft soil (Molas and Yamazaki, 1995). The Zhao *et al.* (2006) models are currently used by the U.S. Geological Survey ShakeMap product for subduction zone settings worldwide, including the ShakeMap for the September earthquakes. We study two distinct implementations of the Zhao *et al.* (2006) GMPE: SS slab and ASC. The functional form for the Zhao *et al.* (2006) model includes terms representing magnitude scaling, geometrical spreading, intrinsic attenuation, hanging-wall effects (for crustal reverse events), an NEHRP site class term, focal depth, and a slab versus interface classification. The inslab classification is a function of distance, to account for complex path effects in slab events.

Finally, we include the BC Hydro GMPE (Table 1) with the inslab characterization (Abrahamson *et al.*, 2016). To develop this GMPE, empirical subduction zone earthquake data from Alaska, Cascadia, Japan, Taiwan, south and central America, and Mexico were used, in addition to simulated earthquake data, out to 300 km distance. Abrahamson *et al.* (2016) found that Japanese events exhibited stronger attenuation in the back-arc region (behind the megathrust volcanic arc) than in the fore-arc region (area between the trench and volcanic arc). The GMPE includes an additional term classifying each site as fore-arc or back-arc; this term is not a site effect, but instead adjusts the ground-motion model. In ad-

dition to the fore-arc/back-arc site term, this GMPE includes linear and nonlinear V_{S30} scaling for site effects. Other terms include magnitude scaling, an uncertainty on the break in magnitude scaling, geometrical spreading as a function of both magnitude and inslab versus interface characterizations, intrinsic attenuation, and hypocentral depth.

The BC Hydro model uses hypocentral distance (R_{hyp}) for the inslab characterization, which implies the fault finiteness of damaging inslab events can be disregarded. They chose to use hypocentral distance because the magnitude of the inslab events is not as high as that of interface events, because of their generally deeper occurrence, and because the many of the events in the BC Hydro dataset have not been modeled. Neither of the first two conditions is satisfied for the two Mexico earthquakes studied here. Both events exhibit nonnegligible fault finiteness: The Tehuantepec earthquake is $\sim 150 \times 80 \text{ km}$ in dimension (Melgar, Ruiz-Angulo, *et al.*, 2018), whereas the Puebla-Morelos earthquake is $\sim 60 \times 30 \text{ km}$ (Melgar, Pérez-Campos, *et al.*, 2018). The other three GMPEs rely on closest distance to rupture (R_{rup}), and for each we use the relevant distance metric. The distance metrics are computed using the source models of Melgar, Ruiz-Angulo, *et al.* (2018) and Melgar, Pérez-Campos, *et al.* (2018). We consider only those parts of the slip model having a minimum of 20% of the peak slip in the entire model.

We determine a proxy V_{S30} value for each site for which we have seismic data, which represents the time-averaged shear-wave velocity in the top 30 m of the surface at a station. We use a global proxy model that relates V_{S30} topographic hill slope (Wald and Allen, 2007; Allen and Wald, 2009). The BC Hydro and Zhao GMPEs include site terms for either nonlinear V_{S30} effects, or site classification dependent on V_{S30} , which we implement. Additionally, we classify each site as either fore-arc or back-arc, for implementation into the BC Hydro GMPE, a distinction that is somewhat straightforward at subduction zones with simple arc structures. However, in Mexico the complex history of flat slab subduction produces a rather unique arc structure (Fig. 1, Ferrari *et al.*, 2012). There is one main volcanic arc oblique to the trench, the Trans-Mexican volcanic belt (TMVB), which extends west to east and terminates abruptly near the Gulf of Mexico

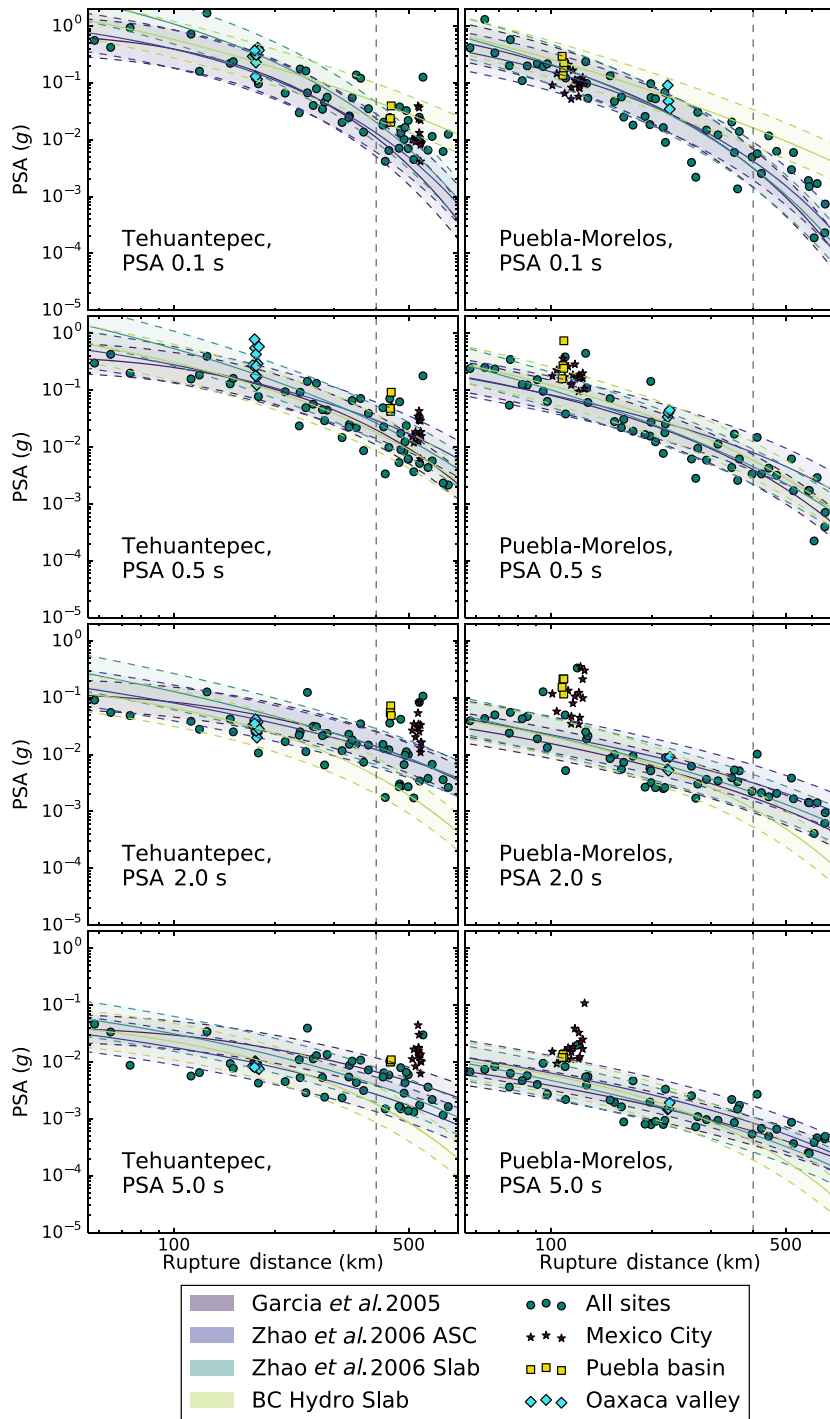


Figure 2. GMPE predictions for four GMPEs for the Tehuantepec and Puebla-Morelos earthquakes, for a hard-rock site ($V_{S30} = 760$ m/s), and assuming a fore-arc site classification (for BC Hydro). Shown here for four periods, pseudospectral acceleration (PSA) 0.1, 0.5, 2.0, and 5.0 s at 5% damping; all periods computed can be found in \textcircled{E} Figures S1 and S2 (available in the electronic supplement to this article). GMPEs are García *et al.* (2005); Zhao *et al.* (2006), active-shallow crust (ASC); Zhao *et al.* (2006), inslab (Slab); and Abrahamson *et al.* (2016), inslab (BC Hydro). Solid lines are GMPE medians; dashed lines show the median plus/minus the standard deviation of each model. Scattered circles are observations of ground motion at all sites; stars are observed ground motions in Mexico City, squares in Puebla, and diamonds in Oaxaca. The vertical dashed line is the farthest distance upon which any of the models were developed (400 km). The color version of this figure is available only in the electronic edition.

coast. Southeast of the TMVB, the volcanism is discontinuous with its only onshore expression being the Los Tuxtlas volcanic field (TVF). Farther south the modern Chiapanecan volcanic arc (MCVA) reflects Miocene and younger volcanism, which is offset from the more traditionally oriented central American volcanic arc (CAVA) in Guatemala and further south. We draw a contour connecting the distal part of each one of these features, which we use as the limit between fore-arc and back-arc (thick dashed line in Fig. 1). This definition yields only a single back-arc site for the Tehuantepec event, and two for the Puebla-Morelos event.

For each earthquake and GMPE, we calculate residuals between observed and predicted ground motions as

$$\delta_{ij} = \ln(Y_{ij,\text{obs}}) - \ln(Y_{ij,\text{pred}}), \quad (1)$$

in which Y is the intensity measure (PGA, or spectral acceleration [SA]) from the GMPE for any earthquake i at station j . We did perform a mixed-effects regression with a bias term to investigate between-event (event-term) and within-event (station-term) residuals. However, because there are only two events and a nearly exact set of stations recording them both, the between-event residuals for each event are centered around 0, and do not provide further insight.

Comparison of Data with GMPE Models

The median values and standard deviations for each GMPE are plotted in Figure 2 for select periods, for the Tehuantepec and Puebla-Morelos earthquakes. Comparisons for all eight common ground-motion intensity parameters are shown in \textcircled{E} Figures S1 and S2 (PGA and seven periods of SA). Qualitatively, the Zhao *et al.* (2006) ASC and Slab, as well as García *et al.* (2005) GMPEs seem to model the Tehuantepec and Puebla-Morelos earthquakes adequately, for uniform site conditions (Fig. 2, and \textcircled{E} Figs. S1 and S2). The BC Hydro predictions for fore-arc stations show stronger attenuation with distance for longer periods than at shorter periods and disagree with the predictions from the other models. Stations within basins and valleys

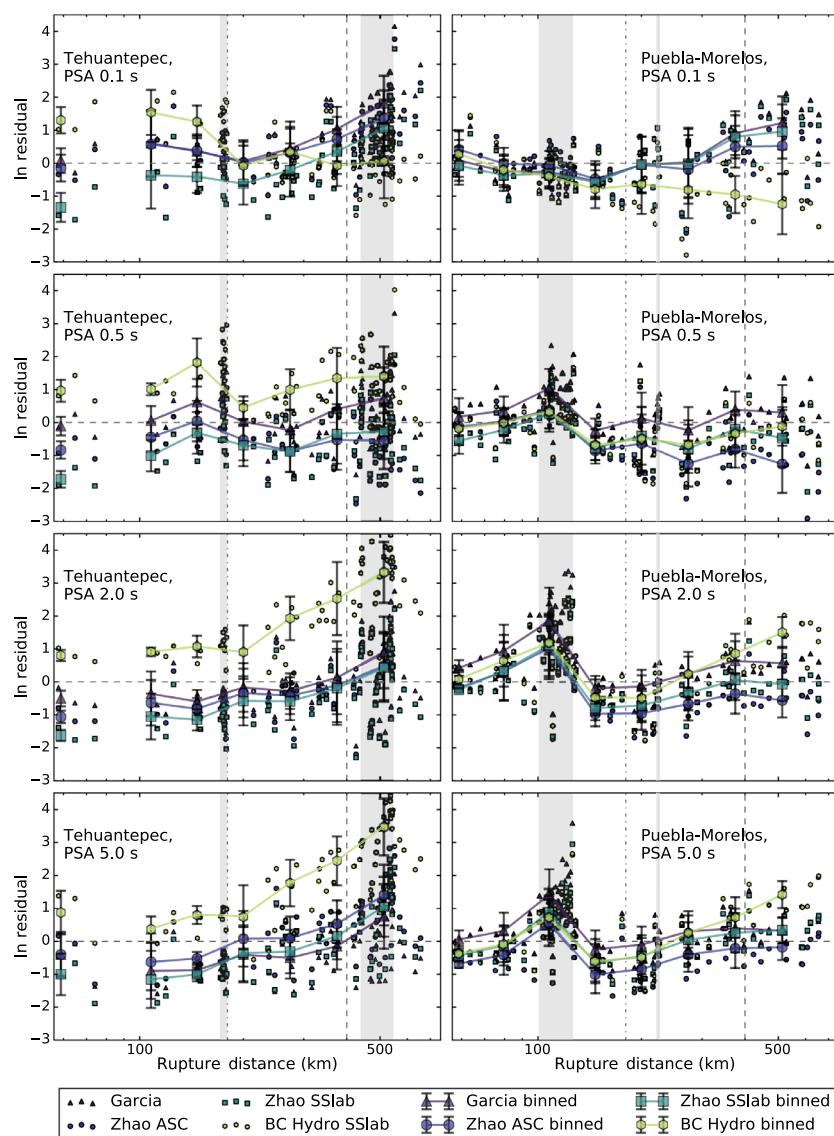


Figure 3. GMPE residuals versus rupture distance for the Tehuantepec Puebla-Morelos earthquakes, at PSA 0.1, 0.5, 2.0, and 5.0 s at 5% damping. Small scattered symbols show each station's residual, with a different symbol for each GMPE; larger symbols with error bars show the binned averages of these residuals, for each GMPE, on nine natural logarithm evenly spaced bins between 55 and 700 km. Triangles: García *et al.* (2005); circles: Zhao *et al.* (2006), ASC; squares: Zhao *et al.* (2006), SSslab; hexagons: BC Hydro. Horizontal dashed line: zero residual; vertical dashed-dotted line: 180 km, distance at which García *et al.* (2009) propose amplification from wedge geometry begins to occur. Vertical dashed line: 400 km, maximum distance for which any of these four GMPEs was developed (400 km). Thick gray hatched area: distance at which Mexico City and Puebla basin stations are for each earthquake. Thin gray double-hatched area: distance at which Oaxaca stations are for each earthquake. The color version of this figure is available only in the electronic edition.

(Mexico City, Puebla, and Oaxaca) consistently show larger ground motions than the models predict; however, this response seems to vary depending on the period.

The model residuals δ_{ij} are plotted for both earthquakes in Figure 3, and *Figures S3 and S4*. Figure 3 shows select periods for both earthquakes. As seen in Figure 2, Figure 3 shows that basin/valley sites are consistently underpredicted

by all ground-motion models, showing positive residuals up to natural log 4 (factor of ~ 55), in some extreme cases. The Tehuantepec earthquake residual binned averages (Fig. 3) generally show a positive trend with distance, in particular at the longer periods. This seems to be exacerbated by the Mexico City and Puebla stations residuals increasing the binned averages at ~ 440 – 540 km. However, even outside this rupture distance range, some periods (i.e., pseudospectral acceleration [PSA] 2.0 and 5.0 s) show negative residuals at the shorter distances, increasing at the greater distances. The BC Hydro GMPE severely underpredicts the ground motion at all but the shorter periods ($T > 0.5$ s), at most rupture distances. No GMPE shows an adequate representation of the attenuation observed for this event at the longer periods. At the near-source distances, there is a significant scatter in the residuals of this event, particularly between models.

The total residuals for the Puebla-Morelos event are also in Figure 3 (see also *Figures S3 and S4* for all). All models perform similarly at each period; these GMPEs generally estimate ground motion well for this event, within the rupture distance on which the models were developed. At periods longer than 0.5 s, however, there is a peak in the residual binned averages for every model at ~ 100 km distance. These residuals are from the Mexico City and Puebla stations, indicating that there is amplification in these regions at predominant periods longer than 0.5 s. Near-source stations are well modeled for this event as well.

From Figure 3, it appears that the García *et al.* (2005) has the smallest absolute value of residual binned averages, at many rupture distances and periods. It is the only GMPE developed for inslab events in Mexico, in particular. Because of its better performance, we show the García *et al.* (2005) residuals in map view

for each earthquake, for PSA 2.0 (Fig. 4) and 0.5 s (Fig. 5). For both the Tehuantepec and Puebla-Morelos earthquakes, stations closer to the Pacific coast systematically show negative residuals, or overprediction. Stations within the TMVB generally show positive residuals or underprediction. At PSA 2.0 s, the Mexico City and Puebla regions show large positive residuals for both earthquakes (greater than the surrounding regions), and at PSA 0.5 s the Oaxaca valley shows

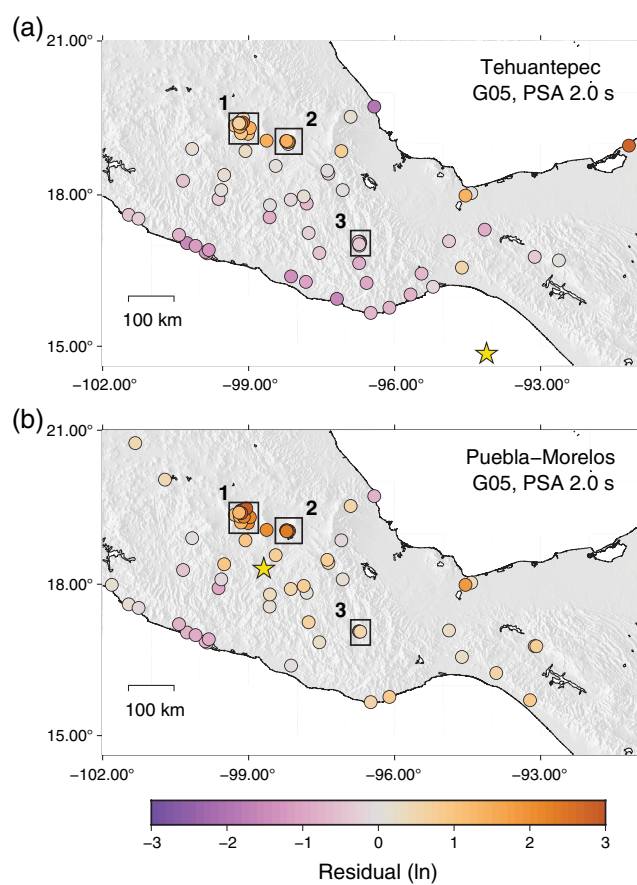


Figure 4. Map view of total residuals for García *et al.* (2005), spectral acceleration (SA) 2.0 s. (a) Residuals for Tehuantepec; (b) residuals for Puebla–Morelos. Boxes marked 1, 2, and 3 are the Mexico City, Puebla, and Oaxaca regions, and are the approximate extent of Figures 6 and 7. The star in each panel shows the epicenter of the earthquake for which the residuals are computed. The color version of this figure is available only in the electronic edition.

positive residuals, greater than surrounding stations, for both earthquakes but in particular for Tehuantepec.

To show these basin residuals in detail, we plot the residuals in the inset regions in Figures 6 and 7, for two periods. Residuals in Mexico City and Puebla at long periods (i.e., 2.0 s) are very large from both earthquakes (Figs. 6 and 7); in some cases, natural logarithm (ln) residuals greater than 3, a factor of 20, are observed at some stations, especially those within the ancient Texcoco Lake region in Mexico City (thick contour). The residuals in these two cities are also large at 0.5 s period, but not as great as the longer periods. At PSA 2.0 s, the Puebla–Morelos earthquake shows greater residuals in Mexico City and Puebla than the Tehuantepec earthquake; at PSA 0.5 s, the residuals are comparable in both cities for these two events. This is not necessarily indicative of the ground motions themselves being larger, but that the relative difference between observed and predicted ground motions is greater for this event. Stations in Oaxaca do not show amplified ground motions at 2.0 s during either the Tehuantepec or Puebla–

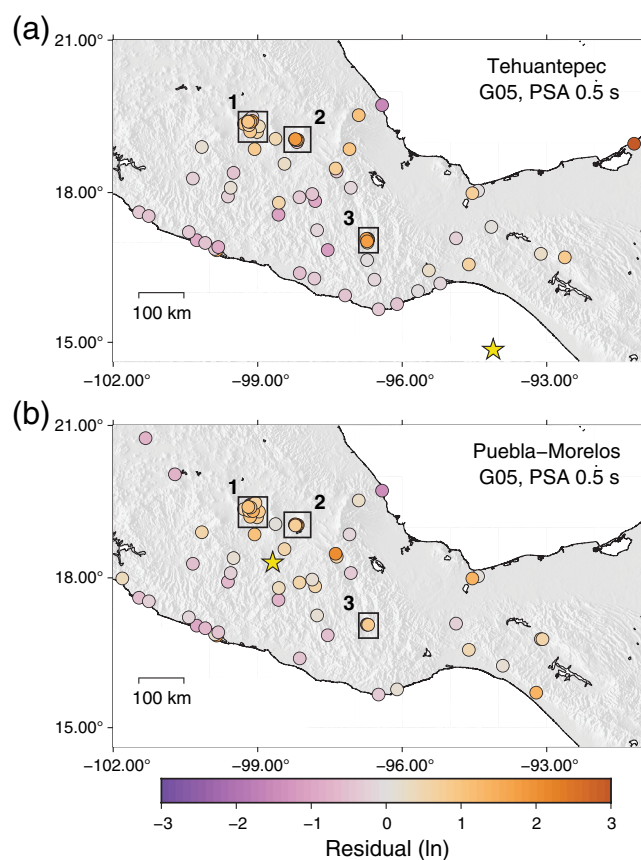


Figure 5. Map view of total residuals for García *et al.* (2005), SA 0.5 s. (a) Residuals for Tehuantepec; (b) residuals for Puebla–Morelos. Boxes marked 1, 2, and 3 are the Mexico City, Puebla, and Oaxaca regions, and are the approximate extent of Figures 6 and 7. The star in each panel shows the epicenter of the earthquake for which the residuals are computed. The color version of this figure is available only in the electronic edition.

Morelos earthquake (Fig. 6), but at 0.5 s period, however, there are moderately large residuals in Oaxaca during the Tehuantepec earthquake (Fig. 7).

Qualitatively, the standard deviations of residuals appear to vary with distance, for each period and earthquake (Fig. 3). We explore the overall observed standard deviations of residuals for each earthquake at various periods (Fig. S5; Table S3). Overall, the standard deviations of the residuals from all four models are similar for either of the earthquakes individually. The exception is the case of the Tehuantepec event at long periods modeled with BC Hydro, which has much larger uncertainty (Fig. S5a). Although similar for individual events, the standard deviations vary more between earthquakes. The residual standard deviations are generally larger for the Tehuantepec earthquake per period, but this is likely because the basin effects at the greater distances/longer periods, exacerbating attenuation values. For the Puebla–Morelos earthquake, there is a significant peak in uncertainty for all models at SA 2.0 s (Fig. S5b), likely because of basin effects from Mexico City and Puebla, as these standard deviations are computed across all distances.

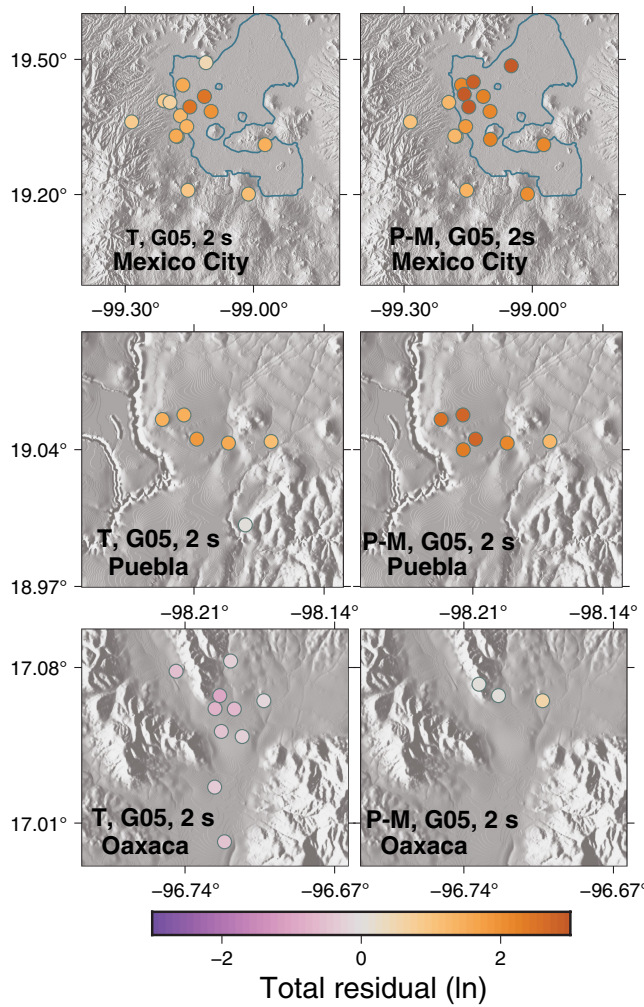


Figure 6. Residuals for the Tehuantepec and Puebla-Morelos earthquakes (labeled P-M and T, respectively) at inset regions, García *et al.* (2005), SA 2.0 s, approximate locations shown in Figures 4 and 5. The thin line in Mexico City is the edge of the ancient lake Texcoco. The color version of this figure is available only in the electronic edition.

Discussion

Model Agreement

Residuals for these two earthquakes show that there is no GMPE that models the observed ground motions well at all periods or at all distances. Between GMPEs, there is always some trade-off between these variables. From here on, we refer to the ensemble average as the qualitative average of residual binned averages, across all four models. In the case of the Puebla-Morelos earthquake, the ensemble average of the four GMPEs performs satisfactorily at most periods and distances; it has low between-model variability, and the residuals are generally close to zero, with the exception of basin sites. This good fit between observed and predicted ground motions begins to decay at the higher frequencies and longer distances (Fig. 3 and Fig. S4), specifically past the maximum model development distance.

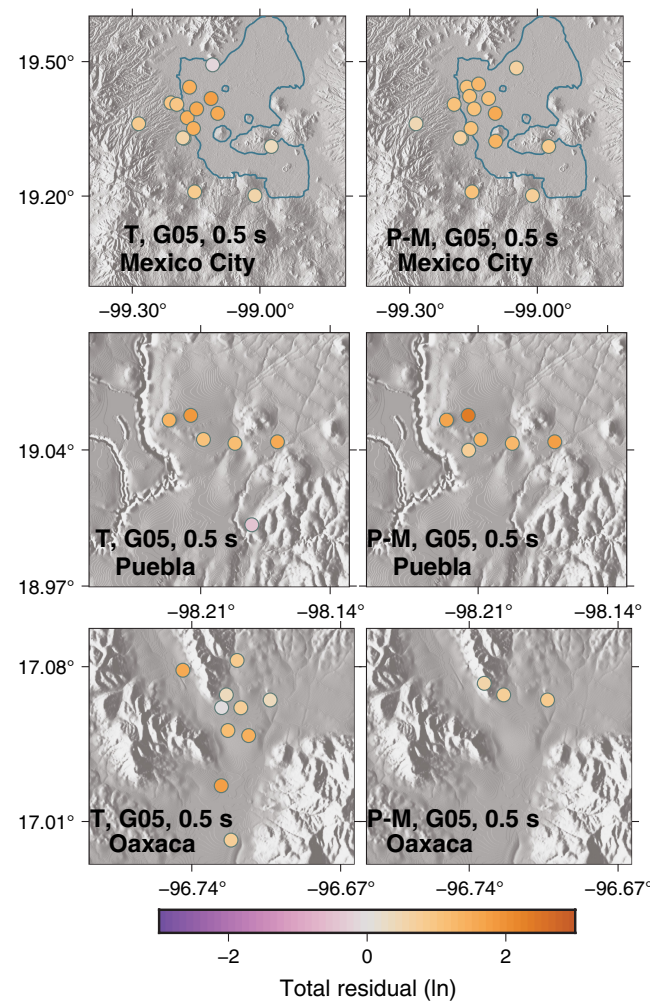


Figure 7. Residuals for the Tehuantepec and Puebla-Morelos earthquakes at inset regions, García *et al.* (2005), SA 0.5 s, approximate locations shown in Figures 4 and 5 (here shown for both earthquakes). The thin line in Mexico City is the edge of the ancient lake Texcoco. The color version of this figure is available only in the electronic edition.

In addition to the ensemble average, the scatter in residuals for the Puebla-Morelos event is less across all periods than it is for Tehuantepec. The standard deviation in residuals for each model at a particular period shows that all models have a total uncertainty of less than ~0.9 at most periods, except SA 2.0 s (e.g., Fig. S5 and Table S3). This value of ≤ 0.9 is comparable to (though perhaps slightly larger than) the total uncertainty observed for many GMPEs (Al-Atik *et al.*, 2010; Boore *et al.*, 2014). In contrast, the Tehuantepec earthquake shows greater overall standard deviations, which can be seen from the binned average error bars (Fig. 3), and standard deviation plot (Fig. S5). We suggest that these observations indicate the Puebla-Morelos earthquake is better-modeled than the Tehuantepec earthquake.

The majority of the near-source ($R_{\text{rup}} < 80$ km) ensemble averages of these two earthquakes are near zero, though the Tehuantepec earthquake shows greater variability

in the near-source ensemble averages. This indicates that these events likely have an average stress drop relative to the datasets on which these GMPEs were developed. For the Puebla-Morelos earthquake, the average uncertainty and small residuals allow us to consider it as well modeled. This is not surprising, as it resembles typical inslab events used in developing the GMPEs.

Regional Attenuation and Waveguide Effects

There are regional differences in the ground-motion residuals. These can be observed in Figures 4 and 5, showing the total residuals in map view for both events, at SA 2.0 and 0.5 s, respectively. For both earthquakes, at both periods, the residuals are lower by the Pacific coastline and higher inland. This ground-motion feature has been noted before, especially for the central portion of the Mexican subduction zone (e.g., [Cardenas and Chavez, 2003](#)). Sparse instrumentation, however, has not identified this feature in the southern part of the country where the Tehuantepec earthquake occurred. [García et al. \(2009\)](#) proposed an attenuation model that treats paths directed inland, that is, orthogonal to the trench, differently from paths parallel to the trench or coast. This model proposes different geometric spreading and intrinsic attenuation (Q) for each path type. [García et al. \(2009\)](#) conclude that these differences are the result of strong postcritical SmS reflections and other Lg -type phases favored by the wedge-shaped geometry of the subduction zone. In addition to these reflections, the low-velocity-subducted oceanic crust channels S-wave energy down-dip and then returns it to the continental crust before the intersection with the continental Moho (~180 km from the earthquake source).

These wave propagation effects are consistent with our observations of higher residuals for inland than Pacific coastal sites. Additionally, the ensemble average of residuals for both earthquakes shows a positive trend past ~180 km, for longer periods ($T > 2.0$ s). Detailed numerical modeling by [Furumura and Kennett \(1998\)](#) and [Furumura and Singh \(2002\)](#) concluded that the first-order geometry of the subduction zone leads to these regional wavefield patterns, especially for periods between 0.25 and 5.0 s. These studies focused on the central part of the subduction zone; however, we find his structural interpretation consistent with our observations and suggest that they hold true elsewhere in the country. There is no reason to expect the wedge shape and waveguiding effect to disappear in the Tehuantepec source region, and thus, it may account for some of the large residuals observed for the Tehuantepec earthquake. This event in particular demonstrates substantial moment release occurring within the proposed waveguide produced by the oceanic crust. As the aforementioned numerical modeling studies observed waveguide effects at periods between 0.25 and 5.0 s, this should explain the large residuals we see at longer distances for the Tehuantepec event. The presence of basin effects from Mexico City and Puebla at longer distances

likely compound this waveguide effect, enhancing the residuals at longer distances for this earthquake.

Beyond complicated wavefields from geometric effects, there is substantial heterogeneity in the overriding continental crust. The regional stratigraphic terranes range from carbonate platforms to cretaceous metamorphic rocks (e.g., [Ferrari et al., 2012](#)). Similarly, the seismic attenuation (Q) structure is complex ([Castro and Munguía, 1993](#); [Castro et al., 1994](#); [Domínguez et al., 1997](#); [Yamamoto et al., 1997](#); [Ottemöller et al., 2002](#)). Although this could possibly play an important role in the regional variation, other studies have shown that there is no obvious relationship yet shown between Q , the geologic terranes, and observed ground motions. One notable exception is that there is strong evidence that the comparatively slower velocity volcanic rocks of the TMVB protract the durations of strong shaking (e.g., [Shapiro et al., 1997](#)). Additionally, although regional structure would be a plausible explanation for the regional variations in total residuals, it does not explain the increasing Tehuantepec residual ensemble averages with increasing distance from ~180 km. We therefore propose that just like for inslab events in central Mexico, for the more southerly Tehuantepec event, the regional slab geometry as a waveguide, is a much stronger control. This regional structure amplifies ground motions at inland stations and is also responsible for the low attenuation and large residuals observed at longer distances, for the longer periods. Another possible avenue to pursue to investigate regional variations in attenuation in the slab up-dip versus down-dip directions. This may elucidate variations in regional residuals for the Puebla-Morelos versus Tehuantepec events.

Basin Effects

We posit that unaccounted-for basin effects are a more important source of misfit between observations and models than these regional attenuation differences. In Mexico City, these are very well known and were illustrated by the destruction from the 1985 Michoacán earthquake. The city is built on very low-velocity water-saturated clays from the ancient Texcoco Lake bounded by a hard-rock volcanic complex. This strong impedance contrast leads to seismic amplification of factors of 10–50, at periods between 1.4 and 5.0 s. It also greatly increases the duration of shaking ([Campillo et al., 1988, 1989](#); [Sánchez-Sesma et al., 1988](#); [Singh, Lermo, et al., 1988](#); [Singh, Mena, et al., 1988](#); [Cruz-Atienza et al., 2016](#)). Much of this amplification has been attributed to interactions between the incoming wavefield and resonant frequencies of the basin ([Chávez-García and Salazar, 2002](#)); however, some research suggests that the effects of the basin structure itself may be significant not only on the amplified ground motion but also on the long-duration records (e.g., [Shapiro et al., 2001](#); [Cruz-Atienza et al., 2016](#)).

Our study shows similar results—very large positive residuals in Mexico City, which are particularly prominent at the Lake sites, for both the Tehuantepec and Puebla-Morelos

events (Figs. 6 and 7). For example, station SCT in our study shows a residual of ~ 1.5 (ln units) for PGA, and in a Mexico-City-specific GMPE (Jaimes *et al.*, 2015), shows a residual of ~ 1 for the same period. However, we also see large residuals for the sites within the broader basin but outside of the lake at periods of SA ~ 0.5 s and greater, though Figures 7 and 8 show only SA 2.0 and 0.5 s, respectively. This may be in agreement with existing studies of hill-zone amplification in the region (Ordaz and Singh, 1992). Interestingly enough, the Puebla-Morelos earthquake shows higher total residuals in Mexico City than Tehuantepec. This indicates that the GMPEs underpredict basin effects more for the Puebla-Morelos earthquake in this region than the Tehuantepec event. We suggest that this is due to the variation in the angle of incidence, as some studies have shown that basin effects in Mexico City may be a combination of path and site effects. Other studies in basins worldwide have noted both path and site effects as the cause of basin amplification (Wirth *et al.*, 2018).

In addition to observing large residuals in Mexico City for these earthquakes, we also see large residuals in the city of Puebla for both the Tehuantepec and Puebla-Morelos earthquakes at longer periods (SA < 0.5 s; Figs. 2, 3, 6, and 7). We also observe large residuals for the stations in the city of Oaxaca at SA ~ 0.5 s during both events, though larger for Tehuantepec (Figs. 6 and 7). Puebla lies on a semi-enclosed plain underlain by thick quaternary volcanoclastics from prominent surrounding stratovolcanoes as well as other volcanic rocks from the TMVB (Ferrari *et al.*, 2007). Site studies and microzonation do exist in Puebla (e.g., Chávez-García *et al.*, 1995); however, there are no studies that we are aware of devoted to basin effects within this city. Chávez-García *et al.* (1995) indicates that the dominant period in much of Puebla is between 0.1 and 2.5 s. This loosely agrees with what we observe, though we also note large basin effects (total residuals ~ 3 in units or greater) at greater than 2.0 s in Puebla during the Tehuantepec earthquake, and positive residuals during the Puebla-Morelos event at these periods. Similarly, the city of Oaxaca is built on a low-lying broad valley at 1500 m above sea level, underlain by a mixture of sandstones and cretaceous metamorphic rocks bounded by prominent mountain ranges that crest at 3000 m above sea level (Ferrari *et al.*, 2007). Existing studies on microzonation and site effects in Oaxaca indicate predominant periods between 0.25 and 1 s (Lermo and Chávez-García, 1993; Castro, 1996). For the Tehuantepec event, we observe positive residuals at higher frequencies (SA ~ 0.5 s), similar to the previous microzonation studies.

Overall, the GMPE basin effects we observe at the three cities seem to be more pervasive than previously described in the literature. Large positive residuals in these regions indicate that because the ground-motion models lack appropriate basin effect terms, they do not predict ground-motion intensity well in these regions. Although basin-specific GMPEs exist for Mexico City, some specifically for intermediate-depth intraslab events (Jaimes *et al.*, 2015, 2016), these

models are very localized and will not account for basins on a larger regional scale. The results here suggest that although Mexico City is an archetype of basin effects and is the subject of many studies thereof, basin effects are more ubiquitous and may require a more physics-based approach to account for hazard on a larger scale. Previous analyses of existing GMPEs such as Next Generation Attenuation-West2 (Bozorgnia *et al.*, 2014) used depth to the 1.0 or 2.5 km/s shear-wavespeed boundary as a proxy for basin effects but do not include other details such as basement structure and basin size (Gregor *et al.*, 2014). None of the models considered here incorporate these proxy terms or other basin effect terms. According to the large residuals observed in Mexico City, Puebla, and Oaxaca, the existing V_{S30} or site classification terms are clearly not enough to model the large amplifications observed in these cities. Such large residuals will contribute to the uncertainty of GMPE predictions, and thus hazard models. Therefore, any model used in probabilistic seismic hazard assessment studies for the region should incorporate detailed, physical as well as empirical, basin effect models.

Implications for Risk

Modeling basin effects correctly in ground-motion models is of the utmost importance for translating hazard to risk. Figure 8 demonstrates this, showing a regional map with population density, as well as plots of the median slope in regions of a certain population density (Fig. 8b), and the number of people in each grid cell with a certain slope value (Fig. 8c). Some of the most densely populated, urban regions of Mexico include Mexico City, Puebla, and Oaxaca—they are all shown here to exhibit nontrivial basin effects. This is perhaps not surprising, as Mesoamerican cultures developed around fertile valleys, highly supportive of agriculture and settlement. As a result, the largest number of people and densest populations of people occur in regions of exceptionally low slope ($< 1\%$ slope). We posit that the majority of the population inhabits places where basin effects are highly likely.

Thus, if risk is representative of both hazard and vulnerability, we have shown here that the greatest misrepresentation of ground-motion amplitudes by GMPEs occurs in regions with the largest populations/most densely populated regions. Simply put, if an important reason for designing GMPEs, albeit not the only one, is for evaluating potential ground motions at the locations where people and structures are, then disregarding basin effects seems to be a critical shortcoming, certainly in the case of the Mexican subduction zone. Indeed, current nationwide hazard maps for the country (CFE, 2015) use GMPEs which lack any of the aforementioned complexity—they are corrected afterward for specific urban centers such as Mexico City using reference sites and microzonations, together with spectral ratios, to account for a variety of site effects. The results of this article suggest that waveguide and basin effects observed in this region are a

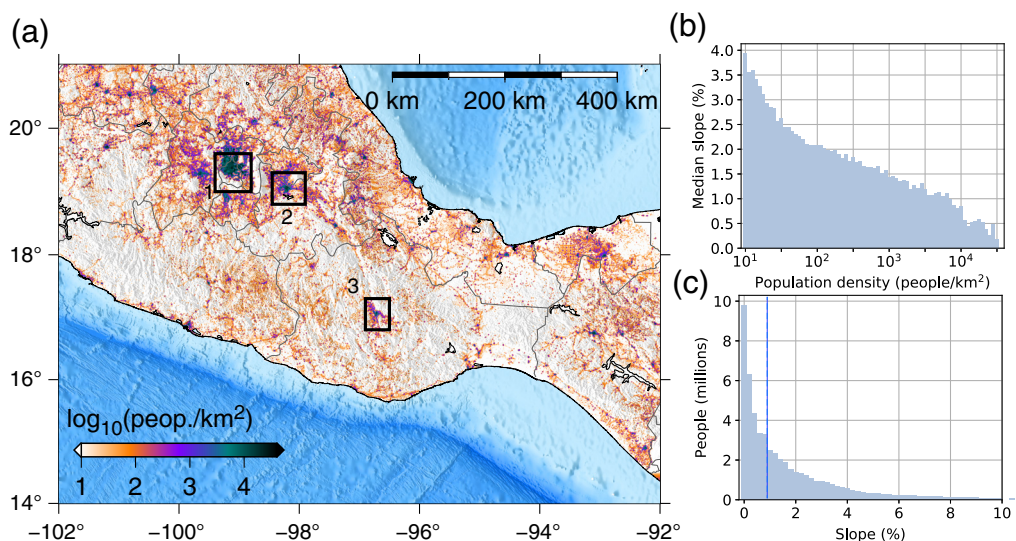


Figure 8. (a) Regional map showing population density. (b) A plot of the median topographic slope in each population density bin in the map (a); this shows that the densest populated regions are also the flattest. (c) Plot of the number of people in each slope bin, the figure shows that 90% of the central part of the country lives in places where slope < 1%. Dashed line, 50th percentile of the population. The color version of this figure is available only in the electronic edition.

strong argument for the development of path-specific nonergodic models, particularly considering the high levels and diversity of seismicity that occurs in Mexico.

In recent years, a number of studies have worked toward site and path-specific (nonergodic) ground-motion models (Landwehr *et al.*, 2016; Kotha *et al.*, 2017), though these have yet to be accepted by the geotechnical community, perhaps because they do not currently account for nonlinear site effects. Because of this, site-specific hazard and risk analyses are complicated endeavors, but would greatly benefit from further work and physics-based inclusions.

Conclusions

By studying the ground motions of the Tehuantepec and Puebla-Morelos earthquakes, we find that the Puebla-Morelos event is generally well modeled by most GMPEs included in this study; most models show small residuals at most periods and distances, and the scatter observed in these residuals is not unlike those proposed for other models worldwide. The Tehuantepec event exhibits stronger regional differences in ground-motion residuals and greater scatter between models. This may be due to a waveguide effect from the subduction zone geometry, including trapped Lg waves and reflected Sms waves, and is less pronounced for the Puebla-Morelos earthquake because of its location as well as the depth to which it ruptured. We find that during both earthquakes, there are very large basin amplification effects in Mexico City and Puebla at periods greater than ~ 1.0 s, and large effects in Oaxaca at higher frequencies (periods < 1.0 s), all of which are not well modeled by the GMPEs. As the majority of the country's population lives in regions underlain by basins, which often correspond with desirable areas of low topographic relief (slope < 1%), understanding

and incorporating more sophisticated basin effects into ground-motion models is critical for improving hazard and risk assessment in the country, as well as worldwide.

Data and Resources

The ground-motion intensity data presented here can be found in [Tables S1 and S2](#) (available in the electronic supplement to this article) for the Tehuantepec and Puebla-Morelos events, respectively. The analysis was performed using Python and maps generated using Generic Mapping Tools (GMT). Strong-motion data from Red Sísmica del Valle de México (RSVM), Servicio Sismológico Nacional (SSN). The data are available by sending an email request to luisq@igeofisica.unam.mx and SSNdata@sismologico.unam.mx. Records for the Unidad de Instrumentación Sísmica at the Instituto de Ingeniería are available at <http://aplicaciones.iingen.unam.mx/AcelerogramasRSM/> (last accessed February 2018) and by sending an email request to LRamirezG@iingen.unam.mx.

Acknowledgments

The authors are indebted to Dave Boore and Deb Kane for their helpful discussions of the results and implications presented in this article. The authors sincerely thank Dave Boore and Jack Boatwright for their thorough and constructive internal reviews of the article. Associate Editor Fabrice Cotton and three anonymous reviewers provided invaluable comments that improved the article. The data used in this work were provided by the Red Sísmica del Valle de México (RSVM), Servicio Sismológico Nacional (SSN, Mexican National Seismological Service), and Unidad de Instrumentación Sísmica (UIS) at the Instituto de Ingeniería (II), Universidad Nacional Autónoma de México (UNAM, National Autonomous University of Mexico). For station maintenance, data acquisition, and distribution, thanks to personnel of SSN and UIS. Financial support for RSVM is provided by Consejo Nacional de Ciencia y Tecnología (CONACYT, National Council for Science and Technology), UNAM, and Gobierno de la Ciudad de México.

(Mexico City Government). V. Sahakian conducted this work while on a Mendenhall Postdoctoral Fellowship, funded by Pacific Gas and Electric (PG&E). Any use of trade, firm, or product names is for descriptive purposes only and does not imply endorsement by the U.S. Government.

References

- Abrahamson, N., N. Gregor, and K. Addo (2016). BC Hydro ground-motion prediction equations for subduction earthquakes, *Earthq. Spectra* **32**, no. 1, 23–44.
- Abrahamson, N. A., and W. J. Silva (1997). Empirical response spectral attenuation relations for shallow crustal earthquakes, *Seismol. Res. Lett.* **68**, 94–127.
- Al Atik, L., N. Abrahamson, J. J. Bommer, F. Scherbaum, F. Cotton, and N. Kuehn (2010). The variability of ground-motion prediction models and its components, *Seismol. Res. Lett.* **81**, no. 5, 794–801.
- Allen, T. I., and D. J. Wald (2009). On the use of high-resolution topographic data as a proxy for seismic site conditions (V_{S30}), *Bull. Seismol. Soc. Am.* **99**, no. 2A, 935–943.
- Arroyo, D., D. García, M. Ordaz, M. A. Mora, and S. K. Singh (2010). Strong ground-motion relations for Mexican interplate earthquakes, *J. Seismol.* **14**, 769–785.
- Baltay, A. S., and J. Boatwright (2015). Ground-motion observations of the 2014 South Napa earthquake, *Seismol. Res. Lett.* **86**, no. 2A, 355–360.
- Boore, D. M. (2010). Orientation-independent, nongeometric-mean measures of seismic intensity from two horizontal components of motion, *Bull. Seismol. Soc. Am.* **100**, no. 4, 1830–1835.
- Boore, D. M., J. P. Stewart, E. Seyhan, and G. M. Atkinson (2014). NGA-West2 equations for predicting PGA, PGV, and 5% damped PSA for shallow crustal earthquakes, *Earthq. Spectra* **30**, no. 3, 1057–1085.
- Bozorgnia, Y., N. Abrahamson, L. A. Atik, T. D. Ancheta, G. M. Atkinson, J. W. Baker, A. Baltay, D. M. Boore, K. W. Campbell, B. S. J. Chiou, et al. (2014). NGA-West2 research project, *Earthq. Spectra* **30**, no. 3, 973–987.
- Building Seismic Safety Council (BSSC) (2004). *NEHRP Recommended Provisions for Seismic Regulations for New Buildings and Other Structures (FEMA 450)*, Part 1. Provisions; Part 2. Commentary, 2003 Edition, Building Seismic Safety Council for the Federal Emergency Management Agency, Washington, D.C.
- Campillo, M., P. Y. Bard, F. Nicollin, and F. Sánchez-Sesma (1988). The Mexico earthquake of September 19, 1985—The incident wavefield in Mexico City during the Great Michoacán earthquake and its interaction with the deep basin, *Earthq. Spectra* **4**, 591–608, doi: [10.1193/1.1585492](https://doi.org/10.1193/1.1585492).
- Campillo, M., J. C. Gariel, K. Aki, and F. J. Sanchez-Sesma (1989). Destructive strong ground-motion in Mexico City: Source, path, and site effects during great 1985 Michoacan earthquake, *Bull. Seismol. Soc. Am.* **79**, no. 6, 1718–1735.
- Cardenas, M., and F. J. Chavez (2003). Regional path effects on seismic wave propagation in Central Mexico, *Bull. Seismol. Soc. Am.* **93**, no. 3, 973–985.
- Castro, R. R. (1996). Estimates of the site effects in Oaxaca, Mexico using horizontal to vertical spectral ratios, *Geofisc. Int.* **35**, no. 4, 371–375.
- Castro, R. R., and L. Murguía (1993). Attenuation of *P* and *S* waves in the Oaxaca, Mexico, subduction zone, *Phys. Earth Planet. In.* **76**, no. 3, 179–187.
- Castro, R. R., L. Murguía, C. J. Rebollar, and J. G. Acosta (1994). A comparative analysis of the quality factor *Q* for the regions of Guerrero and Oaxaca, Mexico, *Geofisc. Int.* **33**, no. 3, 373–383.
- Çelebi, M., V. J. Sahakian, D. Melgar, and L. Quintanar (2018). The 19 September 2017 M 7.1 Puebla-Morelos earthquake: Spectral ratios confirm Mexico City zoning, *Bull. Seismol. Soc. Am.* doi: [10.1785/0120180100](https://doi.org/10.1785/0120180100).
- Chávez-García, F. J., and L. Salazar (2002). Strong motion in central Mexico: A model based on data analysis and simple modeling, *Bull. Seismol. Soc. Am.* **92**, 3087–3101, doi: [10.1785/0120010231](https://doi.org/10.1785/0120010231).
- Chávez-García, F. J., J. Cuenca, J. Lerma, and H. Mijares (1995). Seismic microzonation of the city of Puebla, Mexico, *Proceedings: Third International Conf. on Recent Advances in Geotechnical Earthquake Engineering and Soil Dynamics*, Vol. II, St. Louis, Missouri, 2–7 April 1995.
- Comisión Federal de Electricidad (CFE) (2015). *Manual de Obras Civiles*, Comisión Federal de Electricidad, Mexico (in Spanish).
- Cruz-Atienza, V. M., J. Tago, J. D. Sanabria-Gómez, E. Chaljub, V. Etienne, J. Virieux, and L. Quintanar (2016). Long duration of ground motion in the paradigmatic valley of Mexico, *Scientific Reports* **6**, 38807, doi: [10.1038/srep38807](https://doi.org/10.1038/srep38807).
- Domínguez, T., C. J. Rebollar, and R. R. Castro (1997). Regional variations of seismic attenuation of *Lg* waves in southern Mexico, *J. Geophys. Res.* **102**, no. B12, 27,501–27,509.
- Esteva, L. (1968). *Bases para la formulación de decisiones de diseño sísmico*, Instituto de Ingeniería, Universidad Nacional Autónoma de México, available at <http://www.iingen.unam.mx/es-mx/BancodeInformacion/USI/Paginas/default.aspx> (last accessed February 2018) (in Spanish).
- Esteva, L. (1970). *Regionalización sísmica de México para fines de Ingeniería*, Instituto de Ingeniería, Universidad Nacional Autónoma de México, available at <http://www.iingen.unam.mx/es-mx/BancodeInformacion/USI/Paginas/default.aspx> (last accessed February 2018) (in Spanish).
- Ferrari, L., D. Morán, and E. González (2007). *Actualización de Mapa Geológico de México escala 1:4,000,000*, Nuevo Atlas Nacional de México, Instituto de Geografía, Universidad Nacional Autónoma de México (in Spanish).
- Ferrari, L., T. Orozco-Esquivel, V. Manea, and M. Manea (2012). The dynamic history of the Trans-Mexican volcanic belt and the Mexico subduction zone, *Tectonophysics* **522**, 122–149.
- Furumura, T., and B. L. N. Kennett (1998). On the nature of regional seismic phases-III. The influence of crustal heterogeneity on the wavefield for subduction earthquakes: The 1985 Michoacan and 1995 Copala, Guerroero, Mexico earthquakes, *Geophys. J. Int.* **135**, no. 3, 1060–1084.
- Furumura, T., and S. K. Singh (2002). Regional wave propagation from Mexican subduction zone earthquakes: The attenuation functions for interplate and inslab earthquakes, *Bull. Seismol. Soc. Am.* **92**, no. 6, 2110–2125.
- García, D., S. K. Singh, M. Herráiz, M. Ordaz, and J. F. Pacheco (2005). Inslab earthquakes of central Mexico: Peak ground-motion parameters and response spectra, *Bull. Seismol. Soc. Am.* **95**, no. 6, 2272–2282.
- García, D., S. K. Singh, M. Herráiz, M. Ordaz, J. F. Pacheco, and H. Cruz-Jiménez (2009). Influence of subduction zone structure on coastal and inland attenuation in Mexico, *Geophys. J. Int.* **179**, no. 1, 215–230.
- García-Acosta, V., and G. Suárez (1996). *Los sismos en la historia de México*, Fondo De Cultura Económica, Mexico City, Mexico, 718 pp.
- Gobierno del Distrito Federal (GDF) (2004). *Normas Técnicas Complementarias para Diseño por Sismo*, October, Gobierno del Distrito Federal, Mexico City, Mexico (in Spanish).
- Gregor, N., N. A. Abrahamson, G. M. Atkinson, D. M. Boore, Y. Bozorgnia, K. W. Campbell, B. S. J. Chiou, I. M. Idriss, R. Kamai, E. Seyhan, et al. (2014). Comparison of NGA-West2 GMPEs, *Earthq. Spectra* **30**, no. 3, 1179–1197.
- Hayes, G. P., D. J. Wald, and R. L. Johnson (2012). Slab1.0: A three-dimensional model of global subduction zone geometries, *J. Geophys. Res.* **117**, no. B01302, doi: [10.1029/2011JB008524](https://doi.org/10.1029/2011JB008524).
- Jaimes, M. A., J. Lerma, and A. D. García-Soto (2016). Ground-motion prediction model from local earthquakes of the Mexico basin at the hill zone of Mexico City, *Bull. Seismol. Soc. Am.* **106**, no. 6, 2532–2544.
- Jaimes, M. A., A. Ramirez-Gaytán, and E. Reinoso (2015). Ground-motion prediction model from intermediate-depth intraslab earthquakes at the hill and lake-bed zones of Mexico City, *J. Earthq. Eng.* **19**, no. 8, 1260–1278.
- Kotha, S. R., D. Bindi, and F. Cotton (2017). From ergodic to region-and site-specific probabilistic seismic hazard assessment: Method development and application at European and Middle Eastern sites, *Earthq. Spectra* **33**, no. 4, 1433–1453.
- Kottke, A. (2017). *arkottke/pyrotid v0.4.1* (Version v0.4.1), Zenodo, doi: [10.5281/zenodo.531850](https://doi.org/10.5281/zenodo.531850).
- Landwehr, N., N. M. Kuehn, T. Scheffer, and N. Abrahamson (2016). A nonergodic ground-motion model for California with spatially varying coefficients, *Bull. Seismol. Soc. Am.* **106**, no. 6, 2574–2583.
- Lerma, J., and F. J. Chávez-García (1993). Site effect evaluation using spectral ratios with only one station, *Bull. Seismol. Soc. Am.* **83**, no. 5, 1574–1594.

- Mayoral-Villa, J. M., T. C. Hutchinson, K. W. Franke, M. Alcaráz, P. Arduino, D. Asimaki, A. Badillo, G. Candia, E. Castaño, J. Dafni, *et al.* (2017). Geotechnical engineering reconnaissance of the 19 September 2017 M_w 7.1 Puebla-Mexico City earthquake, *GEER Association Report No. GEER-055A*, doi: [10.18118/G6JD46](https://doi.org/10.18118/G6JD46).
- Melgar, D., X. Pérez-Campos, L. Ramírez-Guzmán, Z. Spica, V. H. Espíndola, W. C. Hammond, and E. Cabral-Cano (2018). Bend faulting at the edge of a flat slab: The 2017 M_w 7.1 Puebla-Morelos, Mexico earthquake, *Geophys. Res. Lett.* **45**, no. 6, 2633–2641, doi: [10.1002/2017GL076895](https://doi.org/10.1002/2017GL076895).
- Melgar, D., A. Ruiz-Angulo, E. S. García, M. Manea, V. C. Manea, X. Xu, M. T. Ramírez-Herrera, J. Zavala-Hidalgo, J. Geng, N. Corona, *et al.* (2018). Deep embrittlement and complete rupture of the lithosphere during the M_w 8.2 Tehuantepec earthquake, *Nature Geosci.* doi: [10.1038/s41561-018-0229-y](https://doi.org/10.1038/s41561-018-0229-y).
- Molas, G. L., and F. Yamazaki (1995). Attenuation of earthquake ground-motion in Japan including deep focus events, *Bull. Seismol. Soc. Am.* **85**, 1343–1358.
- Okal, E. A., S. H. Kirby, and N. Kalligeris (2016). The Showa Sanriku earthquake of 1933 March 2: A global seismological reassessment, *Geophys. J. Int.* **206**, no. 3, 1492–1514.
- Ordaz, M., and S. K. Singh (1992). Source spectra and spectral attenuation of seismic waves from Mexican earthquakes, and evidence of amplification in the hill zone of Mexico City, *Bull. Seismol. Soc. Am.* **82**, no. 1, 24–43.
- Ottmöller, L., N. M. Shapiro, S. K. Singh, and J. F. Pacheco (2002). Lateral variation of Lg wave propagation in southern Mexico, *J. Geophys. Res.* **107**, no. B1, doi: [10.1029/2001JB000206](https://doi.org/10.1029/2001JB000206).
- Pacheco, J. F., and S. K. Singh (2010). Seismicity and state of stress in Guerrero segment of the Mexican subduction zone, *J. Geophys. Res.* **115**, no. B1, doi: [10.1029/2009JB006453](https://doi.org/10.1029/2009JB006453).
- Pagani, M., D. Monelli, G. Weatherill, L. Danciu, H. Crowley, V. Silva, P. Henshaw, L. Butler, M. Nastasi, L. Panzeri, *et al.* (2014). OpenQuake engine: An open hazard (and risk) software for the global earthquake model, *Seismol. Res. Lett.* **85**, no. 3, 692–702.
- Pardo, M., and G. Suárez (1995). Shape of the subducted Rivera and Cocos plates in southern Mexico: Seismic and tectonic implications, *J. Geophys. Res.* **100**, no. B7, 12,357–12,373.
- Pérez-Campos, X., Y. Kim, A. Husker, P. M. Davis, R. W. Clayton, A. Iglesias, J. F. Pacheco, S. K. Singh, V. C. Manea, and M. Gurnis (2008). Horizontal subduction and truncation of the Cocos plate beneath central Mexico, *Geophys. Res. Lett.* **35**, L18303, doi: [10.1029/2008GL035127](https://doi.org/10.1029/2008GL035127).
- Pozos-Estrada, A., R. Gómez Martínez, and H. Hong (2014). Desagregación del peligro sísmico para algunos sitios seleccionados de México, *Ing. sísmica* **91**, 31–53 (in Spanish).
- Sánchez-Sesma, F., S. Chávez-Pérez, M. Suárez, M. A. Bravo, and L. E. Pérez-Rocha (1988). The Mexico earthquake of September 19, 1985—On the seismic response of the Valley of Mexico, *Earthq. Spectra* **4**, 569–589, doi: [10.1193/1.1585491](https://doi.org/10.1193/1.1585491).
- Shapiro, N. M., M. Campillo, A. Paul, S. K. Singh, D. Jongmans, and F. J. Sanchez-Sesma (1997). Surface-wave propagation across the Mexican volcanic belt and the origin of the long-period seismic-wave amplification in the Valley of Mexico, *Geophys. J. Int.* **128**, 151–166.
- Shapiro, N. M., S. K. Singh, D. Almora, and M. Ayala (2001). Evidence of the dominance of higher-mode surface waves in the lake-bed zone of the Valley of Mexico, *Geophys. J. Int.* **147**, no. 3, 517–527.
- Shedlock, K. M. (1999). Seismic hazard map of north and central America and the Caribbean, *Ann. Geofis.* **42**, no. 6, 977–997.
- Singh, S. K., J. Lermo, T. Dominguez, M. Ordaz, J. M. Espinosa, E. Mena, and R. Quaas (1988). The Mexico earthquake of September 19, 1985—A study of amplification of seismic waves in the Valley of Mexico with respect to a hill zone site, *Earthq. Spectra* **4**, 653–673, doi: [10.1193/1.1585496](https://doi.org/10.1193/1.1585496).
- Singh, S. K., E. A. Mena, and R. Castro (1988). Some aspects of source characteristics of the 19 September 1985 Michoacan earthquake and ground motion amplification in and near Mexico City from strong motion data, *Bull. Seismol. Soc. Am.* **78**, no. 2, 451–477.
- Singh, S. K., M. Ordaz, J. F. Pacheco, R. Quaas, L. Alcántara, S. Alcocer, C. Gutiérrez, R. Meli, and E. Ovando (1999). A preliminary report on the Tehuacan, Mexico earthquake of June 15, 1999 (M_w = 7.0), *Seismol. Res. Lett.* **70**, no. 5, 489–504.
- Singh, S. K., G. Suárez, and T. Domínguez (1985). The Oaxaca, Mexico, earthquake of 1931: Lithospheric normal faulting in the subducted Cocos plate, *Nature* **317**, no. 6032, 56–58.
- Universidad Nacional Autónoma de México (UNAM) Seismology Group (1986). The September 1985 Michoacan earthquakes: Aftershock distribution and history of rupture, *Geophys. Res. Lett.* **13**, 573–576.
- Wald, D. J., and T. I. Allen (2007). Topographic slope as a proxy for seismic site conditions and amplification, *Bull. Seismol. Soc. Am.* **97**, no. 5, 1379–1395.
- Wirth, E., A. Frankel, N. Maraki, J. Vidale, and W. Stephenson (2018). Broad-band synthetic seismograms for M 9 earthquakes on the Cascadia megathrust based on 3D simulations and stochastic synthetics (part 2): Rupture parameters and variability, *Bull. Seismol. Soc. Am.* (in press).
- Yamamoto, J., L. Quintanar, R. B. Herrmann, and C. Fuentes (1997). Lateral variations of Lg coda Q in southern Mexico, *Pure Appl. Geophys.* **149**, no. 3, 575–599.
- Ye, L., T. Lay, Y. Bai, K. F. Cheung, and H. Kanamori (2017). The 2017 M_w 8.2 Chiapas, Mexico, earthquake: Energetic slab detachment, *Geophys. Res. Lett.* **44**, no. 23, 11,824–11,832.
- Zhao, J. X., J. Zhang, A. Asano, Y. Ohno, T. Oouchi, T. Takahashi, H. Ogawa, K. Irikura, H. K. Thio, P. G. Somerville, *et al.* (2006). Attenuation relations of strong ground-motion in Japan using site classification based on predominant period, *Bull. Seismol. Soc. Am.* **96**, no. 3, 898–913.
- Zúñiga, R., G. Suárez, M. Ordaz, and V. García-Acosta (1997). *Seismic Hazard in Latin America and the Caribbean*, Vol. 2, IDRC, Ottawa, Canada, 82 pp.

U.S. Geological Survey Earthquake Science Center
345 Middlefield Road, MS 977
Menlo Park, California 94025
vjs@uoregon.edu
(V.J.S., A.B.)

Department of Earth Sciences
University of Oregon
1585 East 13th Avenue
Eugene, Oregon 97403
(D.M.)

Instituto de Geofísica
Universidad Nacional Autónoma de México
Circuito de la Investigación s/n
Ciudad Universitaria, Coyoacan
04510 Mexico City, Mexico
(L.Q., X.P.-C.)

Instituto de Ingeniería
Universidad Nacional Autónoma de México
Circuito Interior s/n
Ciudad Universitaria, Coyoacan
04510 Mexico City, Mexico
(L.R.-G.)

Manuscript received 13 April 2018;
Published Online 16 October 2018